Environmental Science and Pollution Research (2019) 26:29917–29929
https://doi.org/10.1007/s11356-019-06146-2

RESEARCH ARTICLE

Transformation of phosphorus and stabilization of heavy metals during sewage sludge incineration: the effect of suitable additives and temperatures

Rundong Li[1,2] · Wenchao Teng[1] · Yanlong Li[2] · Jing Yin[2] · Ziheng Zhang[2]

Received: 11 March 2019 / Accepted: 31 July 2019 / Published online: 13 August 2019

Abstract

Phosphorus (P), an irreplaceable nutrient for all living organisms, is facing scarcity via phosphate resources. In this research, the effect of suitable additives and temperature on P and heavy metals speciation during sewage sludge (SS) thermochemical treatment was investigated. The results demonstrated that additives (CaO and MgO) could promote the conversion of non-apatite inorganic phosphorus (NAIP) to apatite phosphorus (AP). X-ray diffraction measurements indicated that the phosphorus mineral phase in sewage sludge ash (SSA) mainly was AP, with addition of MgO and CaO. Moreover, orthogonal testing revealed that the optimal molar ratio of Mg:Ca:P for P recovery as AP was 1:3.5:1 at 750 °C. Risk index results implied that the heavy metals in the phosphorus-enriched SSA have low potential ecological risk. Thermodynamic equilibrium calculations revealed that P reacted with the other metal ions was in the following order: $Ca^{2+} > Mg^{2+} > Al^{3+} > Fe^{3+} > Zn^{2+} > K^{+}$.

Keywords Sewage sludge ash · Phosphorus recovery · Conversion · Environmental assessment · Thermodynamic equilibrium calculations

Introduction

P is a limited resource that cannot be synthesized nor substituted in living organisms as essential nutrient. Some researchers have predicted that phosphate rock, which is used for phosphate fertilizer production, can be exploited for a few generations (Childers et al. 2011; Adam et al. 2009). SS, a by-product from wastewater treatment plants that riches in many nutrients, could be regarded as renewable resources (Wang et al. 2018; Zhang et al. 2017). The nutritional components of SS can be regarded as a manufactured soil conditioner or special agricultural fertilizer if the clean products could be obtained by new clean technologies (Kacprzak et al. 2017; Walter et al. 2006). However, contaminants in SS limit its direct application (Siebielska 2014; Stefaniuk and Oleszczuk 2016). SSA is a by-product from SS incineration plant which riches high concentration phosphate (Schwitalla et al. 2018). Therefore, SSA has significant potential for use as a renewable source of phosphate for production of fertilizers.

P can be classified into five fractions: total phosphorus (TP), organic phosphorus (OP), inorganic phosphorus (IP), none-apatite inorganic phosphorus (NAIP), and apatite phosphorus (AP); the relationship of the different P fractions could be described by the equation TP = IP + OP and IP = NAIP + AP (Pardo et al. 2003). AP (Ca/Mg–P) has higher bioavailability and NIAP (Fe/Al/Mn–P) has low bioavailability. P recovery from SSA is generally divided into two approaches: wet chemical recovery and thermal chemical recovery. Wet chemical recovery refers to the use of acid or alkalis to digest SSA, and then P is recovered using a precipitant agent. Many studies had focused on P recovery via acid leaching. Sulfuric

Responsible editor: Ta Yeong Wu

✉ Rundong Li
rdlee@163.com

[1] School of Environmental Science and Engineering, Tianjin University, Tianjin, China

[2] The Key Laboratory of Clean Energy Liaoning Province, Shenyang Aerospace University, Shenyang, China

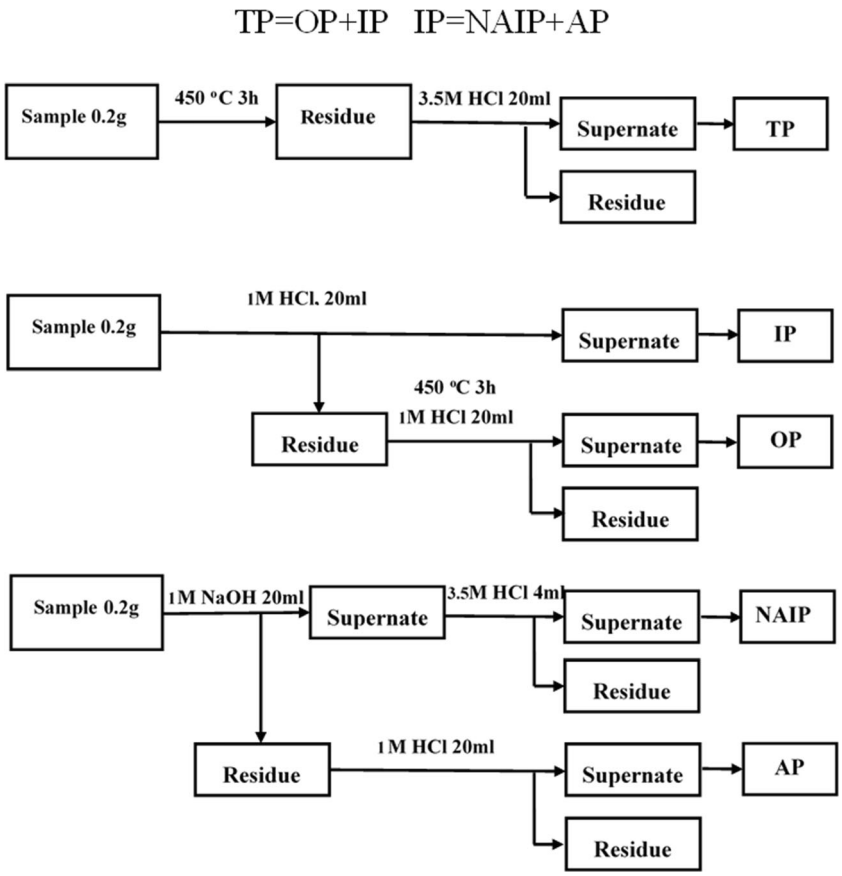

Fig. 1 Phosphorus sequential extraction by SMT extraction protocol

acid (H_2SO_4) and hydrochloric (HCl) are widely used because of their low cost and wide availability, and 60–80% release of P from SSA through leaching (Donatello and Cheeseman 2013). Some researchers also reported that P could be recovered by phosphate precipitation (Xu et al. 2012; Ahmad and Idris 2014). Kong et al. (2018) also reported that Ca plays key role in sorbing P from aqueous solution. Thermal chemical recovery refers to the use of SS incineration processes to enrich P and to promote NAIP conversion to AP to improve P bioavailability. Han et al. (2009) reported that CaO could promote heavy metals and P stabilization in the SSA and high temperatures also could promote conversion between NAIP and AP to form Ca–P (Li et al. 2015; Qian and Jiang 2014; Wang et al. 2013), which has higher bioavailability.

One crucial problem for SS application lies in the content and transformation of heavy metals (Chen et al. 2014; Huang and Yuan 2016). During SS incineration, heavy metal pollutions have caused environmental and regulatory concern because of its toxicity and bioaccumulation (Lia et al. 2016). Most researches on heavy metals in SS thermal treatment are based on heavy metals stabilization or the removal of heavy metals to decrease potential risks to ecosystems (He et al. 2016a, b). Cl donors were beneficial in promoting the heavy metal vaporization during the SS thermal treatment processing

Table 1 Analyses of primary characteristics of the SS

SS	Proximate analysis (wt%, as air-dried)		Ultimate analysis (wt%, as air-dried)	
	M_{ad}	4.2	C_{ad}	42.49
	A_{ad}	21.6	H_{ad}	6.79
	V_{ad}	62.5	N_{ad}	6.63
	FC_{ad}	11.7	S_{ad}	1.22
TP mg g^{-1}	IP mg g^{-1}	OP mg g^{-1}	NAIP mg g^{-1}	AP mg g^{-1}
20.41 ± 1.12	15.24 ± 0.95	1.78 ± 0.15	10.74 ± 2.31	1.6 ± 0.35

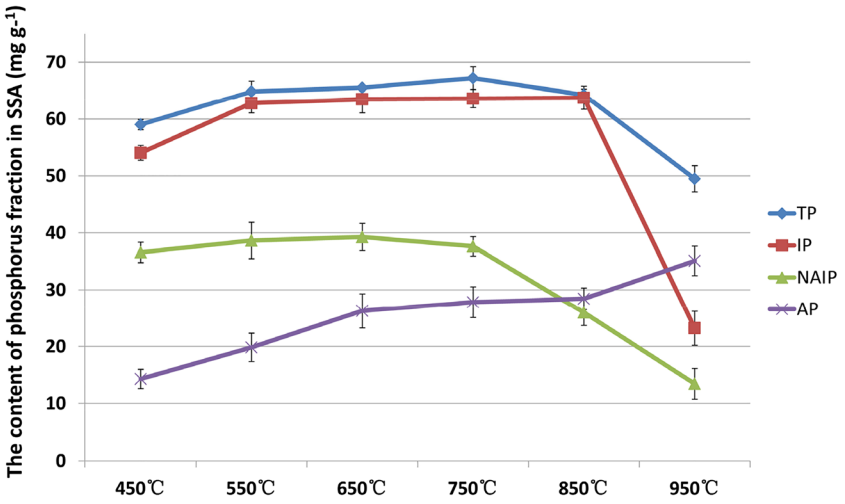

Fig. 2 The content of phosphorus fractions in the SSA at different temperatures without additives

(Li et al. 2015), whereas CaO/MgO and incineration conditions have a positive impact on heavy metal stabilization by promoting heavy metal conversion to aluminosilicate or silicate (Xu et al. 2013). Bairq et al. (2018) also reported that chloride additives, temperature, and residence time could enhance heavy metal removal during SS thermal treatment.

Furthermore, most studies on P recovery are mainly based on wet chemical P recovery from SSA and lack investigation of P fixation, transformation, and bioavailability. The novelty of our research was to convert SSA to phosphate fertilizer directly during SS incineration processes and to avoid using of acids compared with wet chemical P recovery. In addition, some researchers have presented the heavy metal pollution problems but seldom focused on the effect of suitable additives and temperatures on P and heavy metal speciation during SS incineration processes. The purpose of our research was to convert P into a raw material for phosphate fertilizer via suitable additives during SS incineration. An in-depth study on the fractions of heavy metals was conducted to reveal the potential environmental risk from heavy metals of P recovery during SS incineration and the order of P reacted with other metal ions was also investigated.

Materials and methods

Sewage sludge samples

SS samples used in this research were collected from Wastewater Treatment Plant in the city of Dalian, China. SS samples were dried at 105 °C for 2 days within a drum wind drying oven, then crushed by a grinder, sieved to less than 150 μm, and stored in a desiccator.

Incineration experiments

A muffle furnace (air gas atmosphere) was used to investigate the effect of suitable additives and temperature on P and heavy

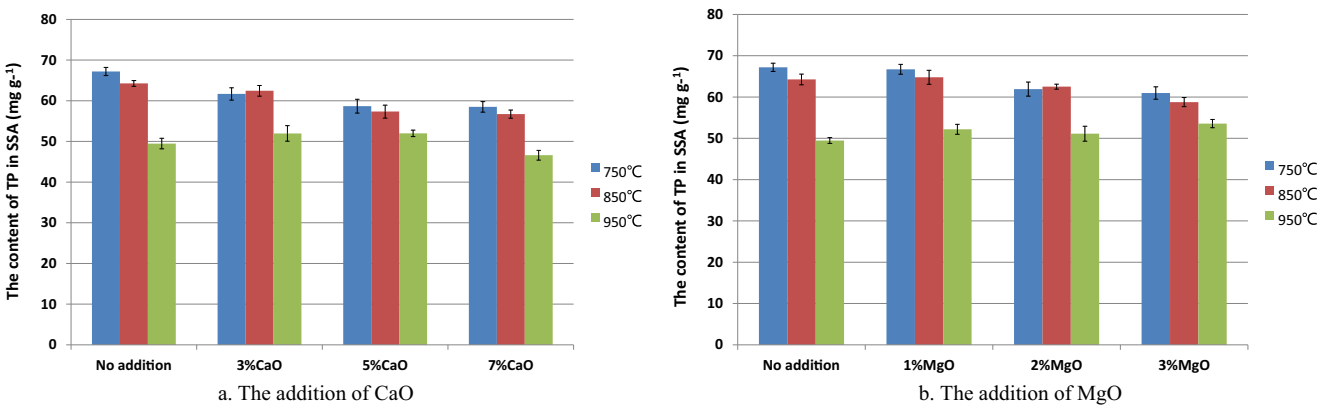

Fig. 3 The influence of temperature and additives on the TP content in SSA. a. The addition of CaO. b. The addition of MgO

metal speciation in the temperature range 450 to 950 °C. In each test, CaO (3, 5, 7 wt%) and MgO (1, 2, 3 wt%) (analytical reagent, Tianjin Kemiou Chemical Reagent Co. Ltd., China) were added to dried SS and homogeneously mixed. Then, the SS samples were burned at setting temperature for 120 min. The SSA was collected, cooled to room temperature in a desiccator, weighed, grinded, and then stored in zip-lock bags for analysis. A 3 × 3 orthogonal test was used to investigate the joint effects of temperature, Mg:P and Ca:P on the P conversion to AP. SSA, with 2 wt% MgO and incinerated at 850 °C, was extracted via alkaline dissolution to attain a residue.

Risk assessment

Potential ecological risk index (RI) and potential ecological risk factor (E_i^r) were used to assess the ecological risks of heavy metals in SSA (Hakanson 1980). The ecological risk of single heavy metal was assessed by E_i^r and the ecological risk of multi heavy metals was assessed by RI. The relationship and calculating methods of RI and E_i^r are expressed in the following equations (Hakanson 1980).

$$E_i^r = T_i^i \times \frac{C_D^i}{C_R^i} \tag{1}$$

$$\mathrm{RI} = \sum_{i=1}^{n} E_i^r \tag{2}$$

E_i^r: the single potential ecological risk factor. T_i^i: the toxic response factor of heavy metals. C_D^i: concentration of single heavy metal in SSA; C_R^i: the reference value for heavy metals. The reference values for heavy metals are in the order of Zn = 80 > Cr = 60 > Ni = 40 > Cu = 30 > As = 15 (He et al. 2016a, b). RI: potential ecological risk index.

Transformation and interaction behaviors of P and heavy metals

Thermodynamic equilibrium calculations were performed in FactSage 6.4 to validate the transformation behaviors of P and the interaction behaviors of P and heavy metals during the SS incineration processes. The materials were input in the form of oxide and were calculated at 750, 850, and 950 °C, respectively.

Analytical methods

In this research, SMT protocol was applied to study the P fractions using a visible spectrophotometer (WFJ2100, UNICO, Shanghai, China) at 882 nm by molybdenum blue method (Kidd et al. 2007) (Fig. 1). The fractions of heavy metals in the SSA was extracted by BCR sequential extraction procedures (Gao et al. 2010). The detailed BCR operation

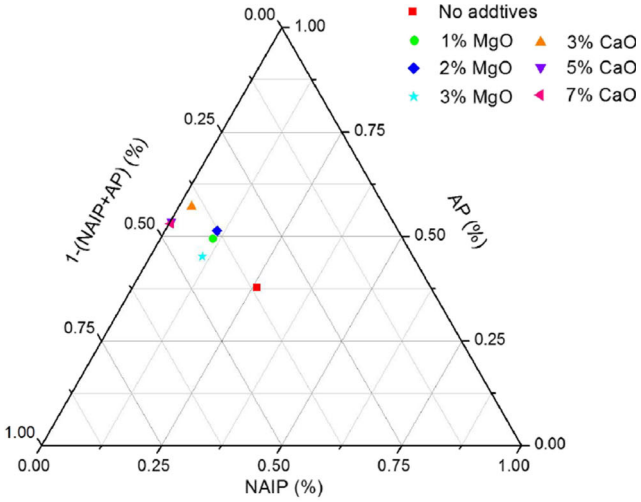

a. Incinerated at 750 °C

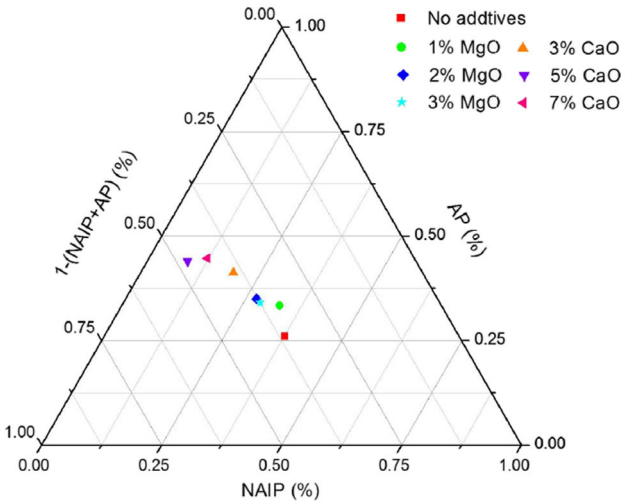

b. Incinerated at 850 °C

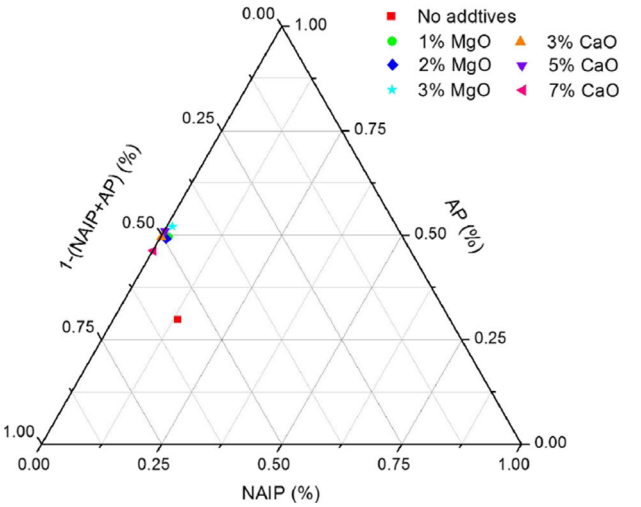

c. Incinerated at 950 °C

◀ **Fig. 4** Ternary plot of the seven investigated SSAs with additives. The values are given as the percentage composition. The prime axes are NAIP and AP. **a** Incinerated at 750 °C. **b** Incinerated at 850 °C. **c** Incinerated at 950 °C

steps could be found in our previous article (Li et al. 2015). Suspensions from BCR sequential extraction procedures were filtered through 0.45-μm membrane by vacuum filter and then stored in polyethylene bottles at 4 °C. The concentration of heavy metals was determined via inductively coupled plasma-atomic emission spectrometry (ICP-OES, PerkinElmer Analyst 8300, USA). The chemical compositions and ultimate analysis of the SS (as shown in Table 1) were examined via X-ray fluorescence (XRF) spectrometer (ZSX100e, MINIFLEX, Japan) and EuroVector Elemental Analyser (EURO ER300, Italy). X-ray diffraction (XRD) was used to identify information on the crystallized phases of the SSA via a PANalytical X'Pert diffractometer (Netherlands). Alkaline dissolution (1 M NaOH) was used to dissolve the non-apatite inorganic phosphorus in SSA. The remained residue was analyzed by XRD to identify the apatite phosphorus.

Results and discussion

A summary of primary characteristics of SS is listed in Table 1. The basic data provided was used to understand the SS properties. As seen in Table 1, SS had high volatile matter content (62.5%). It indicated SS could be ignited easily and could be treated by incinerated to decrease its volume and quality. The TP content in SS was 20.41 ± 1.12 mg g^{-1}. IP, the main fraction of P in SS. The percentage of IP in TP was 75.7%. The percentage of NAIP in IP was 70.5%.

Phosphorus fractions in the SSA obtained at different incineration temperatures

Figure 2 presents the contents of P fractions in the SSA at different incineration temperatures. As shown in Fig. 2, the IP content increased as temperature increased between 450 and 950 °C, reaching its maximum at 850 °C. TP had a similar tendency. AP increased with decreasing NAIP, from 550 to 850 °C, and obviously increased from 25.95 ± 1.37 to 37.77 ± 1.28 mg g^{-1}, from 750 to 850 °C. This indicated the aluminum phosphate (Al–P) belonged to NAIP reacted with the magnesium salt or calcium salt to form the magnesium or calcium phosphate (Mg/Ca–P). Notably, the P fractions decreased in the temperature range of 850 to 950 °C. This phenomenon may be caused by the phase transformation of NAIP and unstable AP. Temperature played an important role in stability of P in SSA, higher temperature led to the phase transformation of some soluble ortho-P and pryo-P which are combined with Al/Fe-compounds (Qian and Jiang 2014).

Phosphorus fractions in the SSA with additives at different incineration temperatures

TP contents in the SSA with additives at different incineration temperatures are presented in Fig. 3. TP did not increase with the presence of additives or with temperature increase. In the contrary, the increasing of additives quality promoted the release of P at the same temperature. The TP content in SSA has the same result with no additives that is obviously decreased at 950 °C. The distributions of P fractions in the SSA are shown in Fig. 4 and indicate different additives had different effects on P transformation. CaO was better than MgO in promoting NAIP conversion to AP (Fig. 4a, b, respectively), as the capacity of P to bind

Table 2 Results of the orthogonal experiment

	T (°C)	Mg:P	Ca:P	TP + AP (mg g^{-1})
1	750	0.5	1.5	112.370 ± 0.782
2	750	1	2.5	114.937 ± 1.364
3	750	1.5	3.5	119.941 ± 1.275
4	850	1	3.5	126.427 ± 0.936
5	850	1.5	1.5	109.719 ± 1.883
6	850	0.5	2.5	102.437 ± 1.273
7	950	1.5	2.5	109.063 ± 0.937
8	950	0.5	3.5	106.822 ± 1.463
9	950	1	1.5	113.476 ± 1.953
$\overline{k1}$	38.58	35.74	37.29	
$\overline{k2}$	37.62	39.43	36.27	
$\overline{k3}$	36.60	37.64	39.24	
Range	1.99	3.69	2.97	

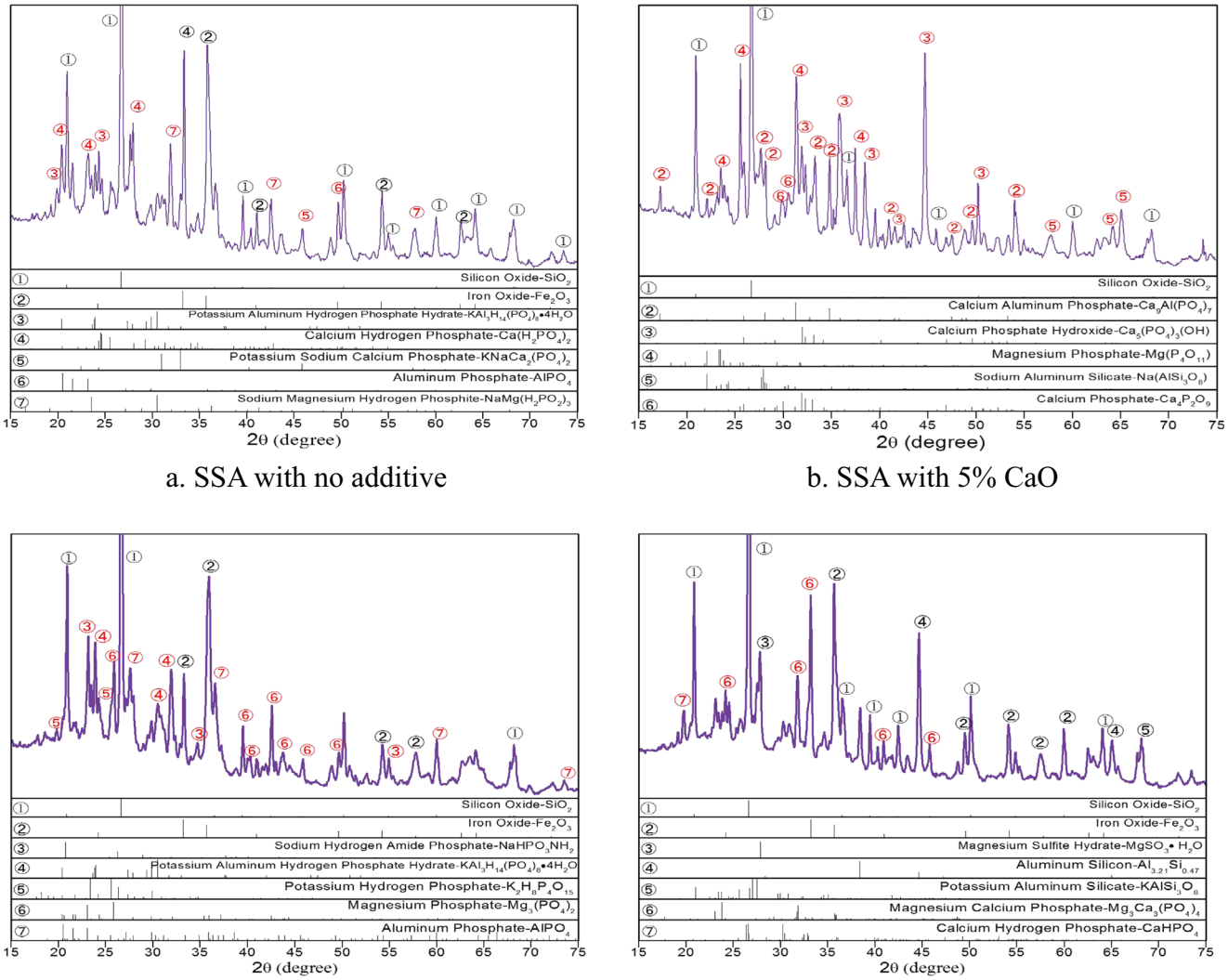

Fig. 5 Mineral analysis of SSA by XRD after incineration at 850 °C. **a** SSA with no additive. **b** SSA with 5% CaO. **c** SSA with 2% MgO. **d** Post-leaching residue from SSA with 2% MgO

Ca^{2+} is better than bind Mg^{2+}, thus forming stable compounds. Gorazda et al. (2012) also reported that calcium could promote the formation of calcium phosphate during SS incineration processing. Han et al. (2009) also reported the similar results. It can be seen that AP did not increase when the Mg:P or Ca:P ratio was greater than or equal to 1. Figure 4 c shows that temperature was the dominant factor for the transformation to AP. The same figure also shows

Table 3 Main crystal phase found in the ash and post-leaching residues via the X-ray method

Crystal phases					Ash incinerated at 850 °C			
					No additive	5% CaO	2% MgO	Post-leaching residue from SSA with 2% MgO
Na,K–P	$NaHPO_3NH_2$						+	
Al–P	$AlPO_4$	$KAl_3H_{14}(PO_4)_8$	$Ca_9Al(PO_4)_7$	NAIP	++	+	++	
Ca–P	$Ca(H_2PO_4)_2$	$CaHPO_4$	$Ca_5(PO_4)_3(OH)$	AP	++	+++		++
Mg–P	$NaMg(H_2PO_2)_3$	$Mg(P_4O_{11})$	$Mg_3(PO_4)_2$	AP	+	+	+	+

One plus sign represents a kind of mineral

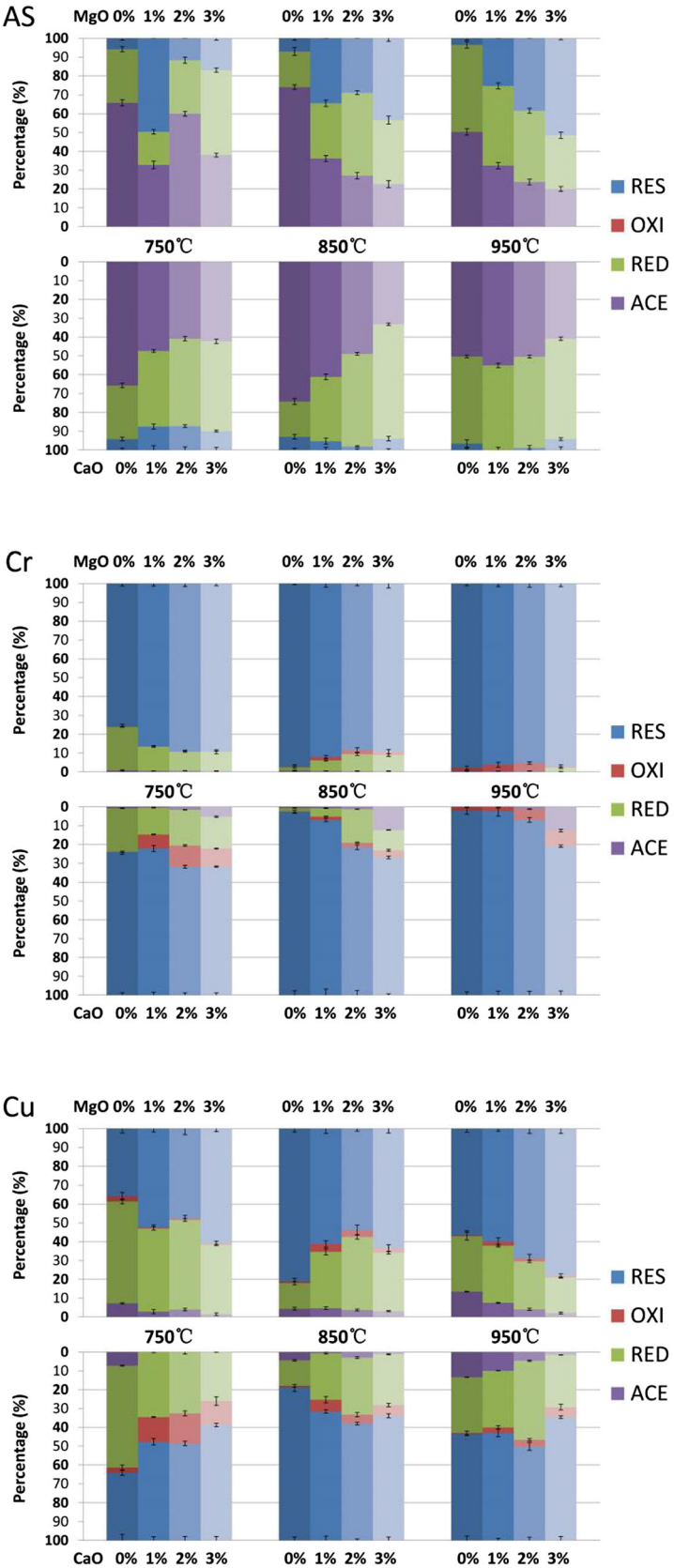

Fig. 6 The distributions of heavy metals in the SSA after incineration with additives at different temperatures

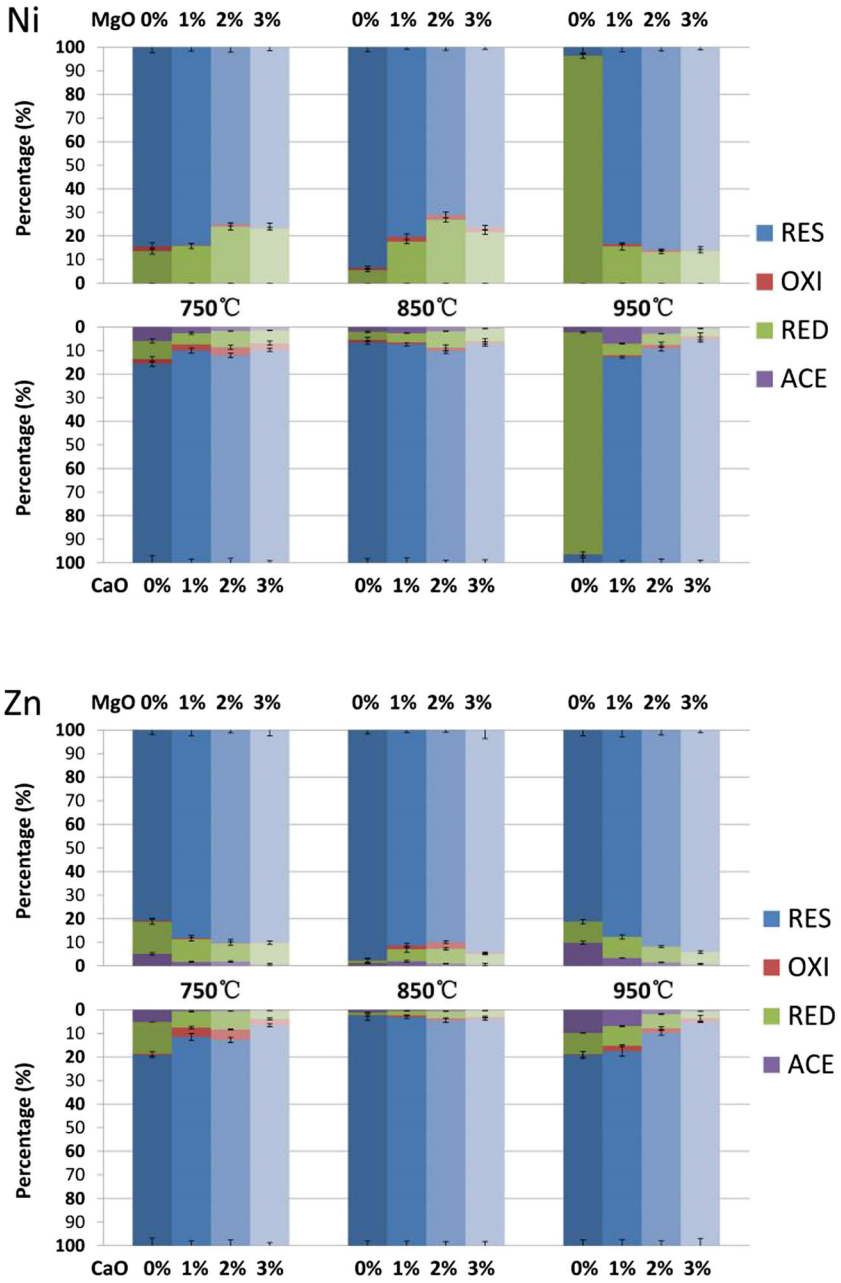

Fig. 6 (continued)

that the content of AP had no direct relationship with the additives at 950 °C. These results illustrated that the additives quality affected the AP at the same temperature and temperature affected the AP at a certain additive quality.

P recovery was based on the formation of AP. To investigate the joint effects of the optimal parameters for P recovery as AP, an orthogonal experiment was conducted (Table 2). Based on the results of the orthogonal texts, the optimal molar ratio of Mg:Ca:P for the precipitation of P as AP was 1:3.5:1 at 750 °C, for a large amount of TP and possible formation of AP. The highest total content of TP+AP reached 126.427 ± 0.936 mg g^{-1} under these conditions, and it can be seen that the parameters influencing the AP formation follows in the order of Mg:P > Ca:P > Temperature.

XRD analyses of the SSA under different conditions

XRD measurements were used to detect the mineral phases, as shown in Fig. 5. Based on the SMT protocol, IP is classified as NAIP and AP. AP (P was bonded with Ca or Al) is the apatite phosphorus which has high bioavailability such as hydroxyapatite, calcium phosphate, and magnesium phosphate. NAIP (P was bonded with Al or

Table 4 Values and corresponding contamination degrees of E_r^i and *RI* in the SSA

	Sample	As E_r^i	Cr E_r^i	Cu E_r^i	Ni E_r^i	Zn E_r^i	RI	
1	750 °C	59.9	4.9	76.4	7.9	12.9	162.1	MR
2	850 °C	46.4	5.2	64.7	9.7	15.2	141.2	LR
3	950 °C	37.5	4.7	61.1	199.0	9.1	311.2	CR
4	750 °C + 1%MgO	64.5	6.9	82.5	12.0	18.1	183.9	MR
5	750 °C + 2%MgO	40.4	4.9	65.9	10.1	14.1	135.4	LR
6	750 °C + 3%MgO	26.9	4.5	47.6	8.4	12.1	99.5	LR
7	850 °C + 1%MgO	39.3	3.4	47.7	7.0	10.1	107.4	LR
8	850 °C + 2%MgO	39.4	3.0	50.7	7.4	9.6	110.0	LR
9	850 °C + 3%MgO	45.1	4.1	59.9	9.1	12.9	131.1	LR
10	950 °C + 1%MgO	35.4	4.2	54.4	8.0	8.2	110.1	LR
11	950 °C + 2%MgO	43.8	3.6	56.1	8.7	6.4	118.5	LR
12	950 °C + 3%MgO	45.3	4.6	52.8	8.7	5.8	117.3	LR
13	750 °C + 3%CaO	29.1	6.4	69.0	10.8	18.1	133.2	LR
14	750 °C + 5%CaO	26.5	5.9	63.2	10.1	17.1	122.8	LR
15	750 °C + 7%CaO	25.4	4.7	61.6	9.9	16.4	117.9	LR
16	850 °C + 3%CaO	30.9	5.0	55.8	9.6	14.7	116.0	LR
17	850 °C + 5%CaO	27.4	4.2	49.6	7.4	12.1	100.7	LR
18	850 °C + 7%CaO	20.8	3.8	51.4	8.9	13.8	98.6	LR
19	950 °C + 3%CaO	29.4	5.0	50.8	8.7	4.2	98.2	LR
20	950 °C + 5%CaO	28.0	3.7	36.8	5.9	3.6	77.9	LR
21	950 °C + 7%CaO	26.4	5.2	47.1	8.4	7.3	94.3	LR

$E_r^i < 40$ low risk, $40 \le E_r^i < 80$ moderate risk, $80 \le E_r^i < 160$ considerable risk, $160 \le E_r^i < 320$ high risk, $E_r^i \ge 320$ very high risk (Chen et al. 2014)

RI < 150 low risk, 150 ≤ RI moderate risk, 300,150 ≤ RI < 600 considerable risk, RI ≥ 600 very high risk (Huang and Yuan 2016)

Fe) is the non-apatite inorganic phosphorus which has low bioavailability such as aluminum phosphate and iron phosphate. Al–P was detected (Fig. 5a), and Al-P dissipated with emerging Mg–P and Ca–P with MgO and CaO addition, respectively (Fig. 5a–c). The results demonstrated that MgO and CaO promoted NAIP conversion to AP during SS incineration processes. In addition, the kinds of additives influenced AP formation.

Comparing Fig. 5 b and a, a significant peak corresponding to Ca–P (2θ = 45°) appeared. From the XRD analyses shown in Fig. 5a, c, the peak of Ca–P (2θ = 35°) decreased with addition of MgO. With MgO addition, the peaks of Al–P, Na–P, and Mg–P appeared. These changes indicated that MgO destroyed the construction of Ca–P and formed a newly crystalline phosphate. Adding additives during SS thermal processing was found to be more advantageous for P transformation, it was more possible to obtain more Ca–P or Mg–P which has higher bioavailability that was significantly more than SS without CaO or MgO. Comparing Fig. 5 c and d, the Al–P disappeared completely after leaching through alkaline dissolution, and then Ca–P and Mg–P existed in the post-leaching residue. This contradictory finding could be interpreted by assuming that Al–P, a kind of NAIP, was dissolved by the aqueous alkali. The chemical equation for such may be as follows:

$$AlPO_4 + 3OH^- \rightarrow Al(OH)_3 + PO_4^{3-} \quad (3)$$

Table 3 shows the main P-containing crystal phases in the ash and post-leaching residues via XRD measurements. It can be found that the newly formed Ca–P is amorphous. Based on these results, CaO or MgO could promote the transformation of aluminum phosphate or iron phosphate to calcium phosphate hydroxide, calcium phosphate, calcium hydrogen phosphate, and finally existed in the SSA in the form of apatite phosphorus. The results presented in this section could provide a basis for P recovery from SSA.

Heavy metal speciation

Figure 5 shows the heavy metal speciation fractions under different incineration conditions obtained via BCR sequential extraction. Based on BCR, heavy metals can be divided into an acid soluble (ACE) fraction, a reducible (RED) fraction, an oxidizable

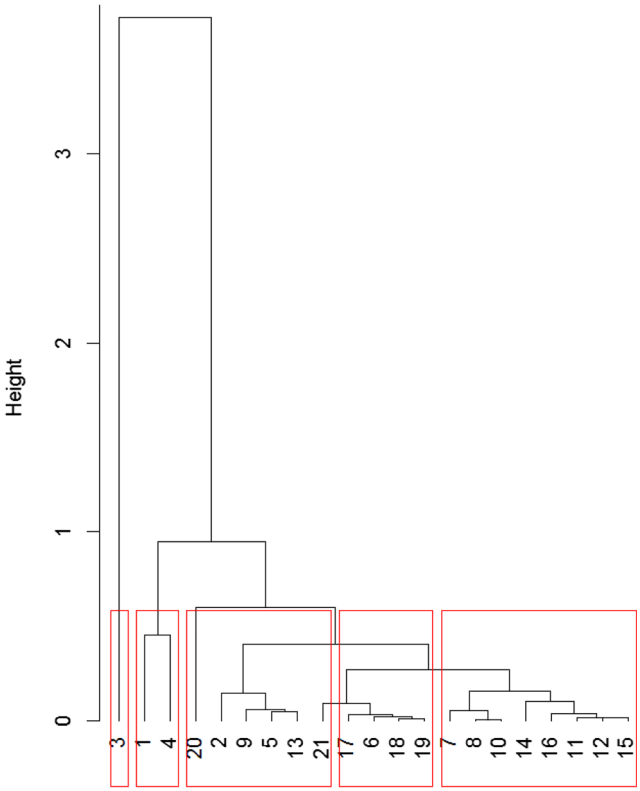

Fig. 7 Dendrogram obtained by hierarchical clustering analyses of the RI values

(OXI) fraction, and a residue (RES) fraction. As shown in Fig. 6, temperature obviously influenced heavy metal fractions, inducing strong migration behavior of the metals. The percentage of the RED fraction was low enough to be considered negligible, except for that of As. At 850 °C, the main fraction of Cr, Cu, Ni, and Zn is the RES fraction, which respectively accounted for 97.3%, 81.2%, 93.5%, and 97.6%, exhibiting low biotoxicity. At 950 °C, for Cu, Ni, and Zn, the percentage of the RES fraction obviously decreased with the percentage of its ACE and RED fractions increased, especially for Ni, whose percentage of RED fraction increased by 90.6%. This may be due to Ni being at non-volatile heavy metal, as higher temperature increased its activity for easy reaction with other ions. As keeps its unique mobility characteristic, higher temperature cannot increase RES fraction of As, the sum of ACE and RED fractions is over 92.9%. Due to ACE and RED, fractions have a high mobility and high biotoxicity (Shi et al. 2013; Li et al. 2015), it directly limits the SSA application as phosphate fertilizer.

As shown in Fig. 6, the results show that CaO and MgO positively affected the mobility behavior of heavy metals. Additives are helpful for heavy metal migration to stable fractions, especially for As. The percentage of RES fractions of As and Cu increased with MgO addition, reaching to 51.5% and 80.1%, respectively, at 950 °C with 3% MgO. The sum percentage of the ACE and RED fractions of As, Cr, Cu, Ni, and Zn showed decreasing tendencies as additives increased, decreasing to 48.5%, 2.2%, 20.9%, 13.5%, and 5.8%, respectively, at 950 °C with 3% MgO. For Cu, Ni, and Zn, CaO also had similar effects on the migration characteristics of the heavy metals as MgO did; most of heavy metal fractions were changed to stable fractions by adding CaO. Han et al. (2009) also reported that CaO could stabilize heavy metals and the percentage of heavy metals in SSA increased with increasing CaO ratio. These results indicate that MgO/CaO could increase the stable fractions of heavy metals.

Potential ecological risk index assessment analyses

The values and corresponding contamination degrees of risk indices and potential ecological risk index of heavy metals in the SSA are listed in Table 4. The E_i^r of the heavy metals in the SSA were in the order of Cu > As>Zn > Ni > Cr. The E_i^r value for Ni without additives at 950 °C was 199.0, indicating considerable risk. The E_i^r values for As with 0, 1%, and 2% MgO at 750 °C; 0 and 3% MgO at 850 °C; and 2% and 3% MgO at 950 °C were 59.9, 64.5, 40.4, 46.4, 45.1, 43.8, and 45.3 respectively. The E_i^r values for Cu under all conditions, except at 950 °C with 5% CaO, were over 40, revealing moderate risk. These results mean high risk to ecosystems, which should be paid more attention, to evaluate the overall potential ecological risk of the heavy metals in the SSA under different incineration conditions. The RI of heavy metals in the SSA at 950 °C was as high as 311.2, revealing considerable risk. The RI values of heavy metals in the SSA under other incineration conditions were lower than 150, except for the conditions for 0 and 1% MgO at 750 °C (moderate risk), meaning low risk. Similarly, the RI values were also analyzed via clustering methods using R Software and organized in a dendrogram to identify groups that were similar. The results are shown in Fig. 7. The RI values could be grouped into five clusters, with considerable risk cluster with 1 sample, moderate risk cluster with 2 samples, and low risk cluster with 6, 4, and 8 samples. Base on hierarchical clustering analyses of RI values, the SSA obtained with 0% and 1% MgO at 750 °C or at 950 °C with no addition should be paid more attention and heavy metals in the SSA should be further removed if the SSAs were used as phosphate fertilizer. These results are helpful for applications of SSA as phosphate fertilizer. However, high concentrations of heavy metals are over the use limits for agricultural application. Therefore, new methods to decrease heavy metal concentrations should be developed.

Transformation and interaction behaviors of P and heavy metals

Thermodynamic equilibrium calculations were performed with FactSage 6.4 to reveal the transformation and interaction behaviors of P and heavy metals during SS incineration processing. As shown in Fig. 8, when the P content is 0, Cu was

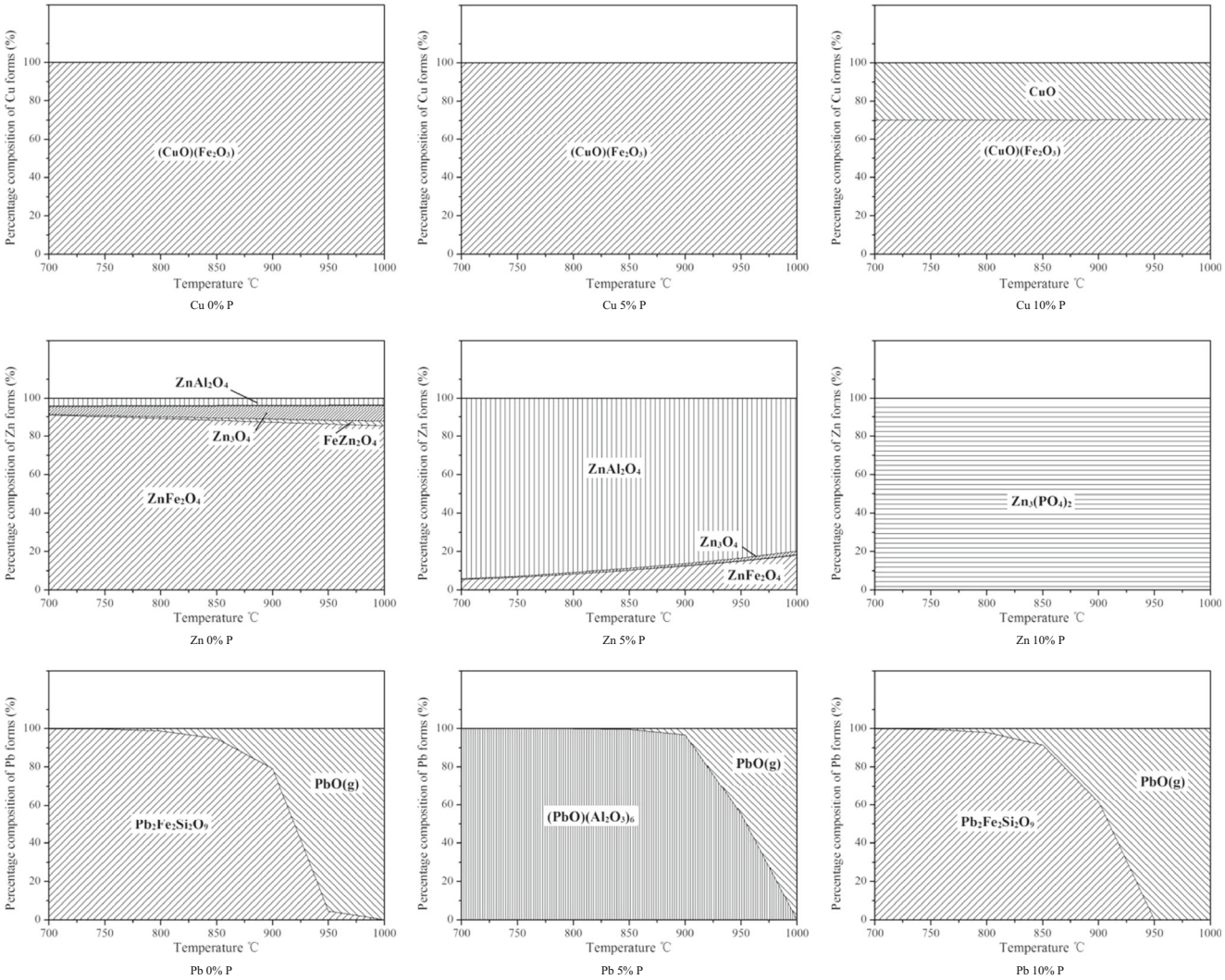

Fig. 8 Results of the thermodynamic equilibrium calculations regarding the influence the different P contents on the forms of heavy metals

in the form of oxide with Fe_2O_3, Zn was mainly in the form of $ZnFe_2O_4$ and $FeZn_2O_4$, and Pb was in the form of $Pb_2Fe_2Si_2O_9$ and $PbO_{(g)}$, the percentage of $PbO_{(g)}$ increased with temperature increasing and was more than 90% at 950 °C; this is due to Zn was greatly influenced by temperature. When the P content increased to 5%, compared to 0% P content, the forms of Zn and Pb changed obviously. Zn was in the form of $ZnAl_2O_4$, with the percentage of $ZnFe_2O_4$ increasing as temperature increased. Pb was in the form of oxide with Al_2O_3. These results indicated that Ca^{2+} and Mg^{2+} firstly combined with P, Fe^{3+} need to combine with Si^{4+}, so heavy metals had to react with Al^{3+} to form heavy metal aluminum compounds. When the P content increased to 10%, Cu was in the form of CuO and $(CuO)(Fe_2O_3)$, Zn reacted with P to form $Zn_3(PO_4)_3$, and Pb was mainly in gaseous form, indicating that excessive amounts of P could promote Pb volatilization.

Figure 9 shows the transformation of P for different percentages of P in the SSA at different temperatures. At 750 °C and 850 °C, first $Ca_5HP_3O_{13}$ was generated, then when phosphorus content increased, the percentage of $Ca_5HP_3O_{13}$ decreased, $Mg_3P_2O_8$ and $Ca_3(PO_4)_2$ were generated. When P content was greater than 5%, $AlPO_4$ was generated and $Ca_5HP_3O_{13}$ disappeared. With P content further increasing, $FePO_4$ and $Zn_3(PO_4)_2$ emerged, and K_2HPO_4 and CaP_2O_6 emerged lastly. At 950 °C, the percentage of Ca–P increased as Mg–P decreased. These results indicated that, at 750 °C and 850 °C, P reacting with other metal ions was in the following order: $Ca^{2+} > Mg^{2+} > Al^{3+} > Fe^{3+} > Zn^{2+} > K^+$. In the actual experiments, NAIP in the SSA was transformed to AP during incineration at higher temperature. This demonstrated that the capacity of combining P and Ca^{2+}/Mg^{2+} is stronger than that of combining P and Al^{3+}/Fe^{3+}, which is similar to the results obtained via thermodynamic equilibrium calculations.

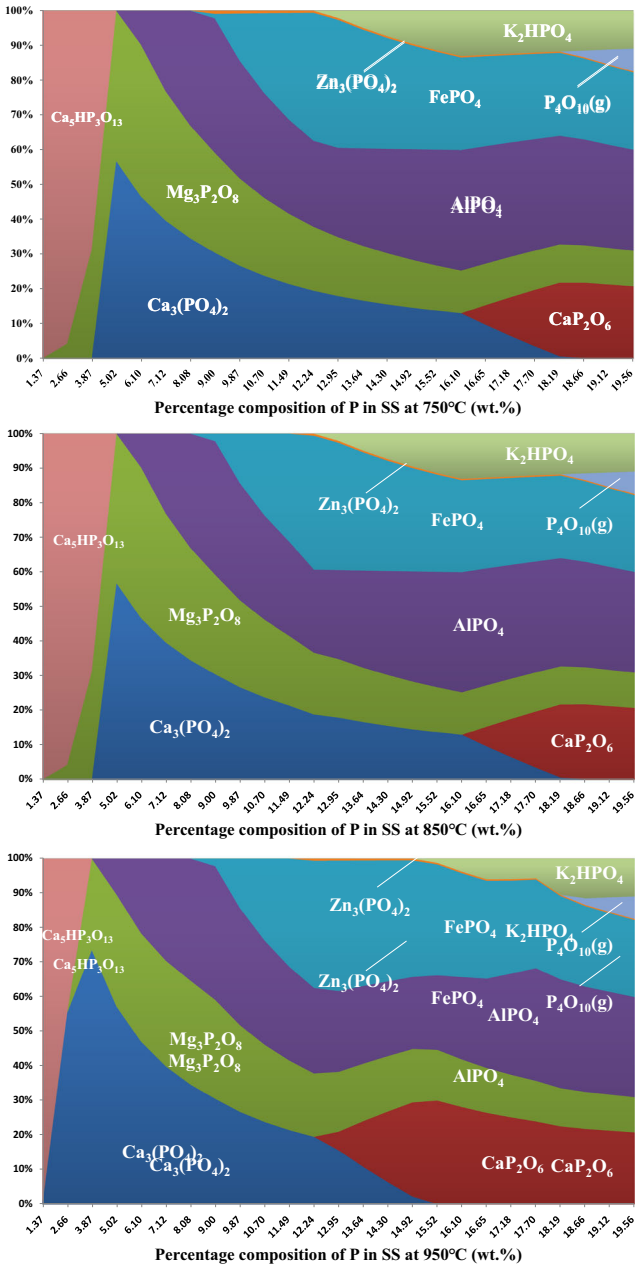

Fig. 9 Thermodynamic calculation of P speciation with different P contents during sewage sludge incineration at different temperatures between 750 and 950 °C

Conclusions

In this research, P potential recovery with different additives during SS incineration was studied to provide a new method for P recovery. MgO and CaO could positively promote the conversion of NAIP to AP. The optimal condition for P recovery as AP was a Mg:Ca:P molar ratio of 1:3.5:1 at 750 °C. The main AP mineral phases in the SSA were $Ca_5(PO_4)_3OH$, $Ca_4P_2O_5$, $Mg_3(PO_4)_2$, $Mg_3Ca_3(PO_4)_4$, and $CaHPO_4$. The additives had a positive influence on heavy metal migration to stable fractions, which had lower biotoxicity. The RI results suggested heavy metals should be removed before sewage sludge incineration, though it showed low risk for the most part. P reacting with other metal ions was in the order: $Ca^{2+} > Mg^{2+} > Al^{3+} > Fe^{3+} > Zn^{2+} > K^+$ during SS incineration processing.

Funding information This work was supported by the National Natural Science Foundation of China, China (No. 51276119 and No. 51576134).

Abbreviations SS, sewage sludge; SSA, sewage sludge ash; TP, total phosphorus; OP, organic phosphorus; IP, inorganic phosphorus; AP, apatite phosphorus; NAIP, non-apatite inorganic phosphorus; Ca/Mg–P, P is associated with Ca or Mg; Al/Fe–P, P is associated with Al or Fe; ACE, acid soluble fraction; RED, reducible fraction; OXI, oxidizable fraction; RES, residue fraction

References

Adam C, Peplinski B, Michaelis M, Kley G, Simon FG (2009) Thermochemical treatment of sewage sludge ashes for phosphorus recovery. Waste Manag 29:1122–1128. https://doi.org/10.1016/j.wasman.2008.09.011

Ahmad AA, Idris A (2014) Release and recovery of phosphorus from wastewater treatment sludge via struvite precipitation. Desalin Water Treat 52:5695–5703. https://doi.org/10.1080/19443994.2013.813101

Bairq ZAS, Li RD, Li YL, Gao HX, Sema T, Teng WC, Kumar S, Liang ZW (2018) New advancement perspectives of chloride additives on enhanced heavy metals removal and phosphorus fixation during thermal processing of sewage sludge. J Clean Prod 188:185–194. https://doi.org/10.1016/j.jclepro.2018.03.276

Chen HC, Zhai YB, Xu BB, Xiang BB, Zhu L, Qiu L, Liu XT, Li CT, Zeng GM (2014) Fate and risk assessment of heavy metals in residue from co-liquefaction of Camellia oleifera cake and sewage sludge in supercritical ethanol. Bioresour Technol 167:578–581. https://doi.org/10.1016/j.biortech.2014.06.048

Childers DL, Corman J, Edwards M, Elser JJ (2011) Sustainability challenges of phosphorus and food: solutions from closing the human phosphorus cycle. Bioscience 61:117–124. https://doi.org/10.1525/bio.2011.61.2.6

Donatello S, Cheeseman CR (2013) Recycling and recovery routes for incinerated sewage sludge ash (ISSA): a review. Waste Manag 33:2328–2340. https://doi.org/10.1016/j.wasman.2013.05.024

Gao X, Chen CTA, Wang G, Xue QZ, Tang C, Chen SY (2010) Environmental status of Daya Bay surface sediments inferred from a sequential extraction technique. Estuar Coast Shelf Sci 86:369–378. https://doi.org/10.1016/j.ecss.2009.10.012

Gorazda K, Kowalski Z, Wzorek Z (2012) From sewage sludge ash to calcium phosphate fertilizers. Pol J Chem Technol 14:54–58. https://doi.org/10.2478/v10026-012-0084-3

Hakanson L (1980) An ecological risk index for aquatic pollution control a sedimentological approach. Water Res 14:975–1001. https://doi.org/10.1016/0043-1354(80)90143-8

Han J, Kanchanapiya P, Sakano T, Mikuni T, Furuuchi M, Wang G (2009) The behaviour of phosphorus and heavy metals in sewage sludge ashes. Int J Environ Pollut 37:357–368. https://doi.org/10.1504/ijep.2009.026054

He XW, Fang ZQ, Wang YX, Jia MY, Song JY, Cheng YJ (2016a) Pollution characteristics, potential ecological risk and health risk assessment of heavy metal in a sewage treatment plant in Beijing. Acta Sci Circumst 36:1092–1098 (In Chinese)

He X, Zhang YX, Shen MC, Zeng GM, Zhou MC, Li MR (2016b) Effect of vermicomposting on concentration and speciation of heavy metals in sewage sludge with additive materials. Bioresour Technol 218:867–873. https://doi.org/10.1016/j.biortech.2016.07.045

Huang HJ, Yuan XZ (2016) The migration and transformation behaviors of heavy metals during the hydrothermal treatment of sewage sludge. Bioresour Technol 200:991–998. https://doi.org/10.1016/j.biortech.2015.10.099

Kacprzak M, Neczaj E, Figalkowski K, Grobelak A, Grosser A, Worwag M, Rorat A, Brattebo H, Almas A, Singh BR (2017) Sewage sludge disposal strategies for sustainable development. Environ Res 156:39–46. https://doi.org/10.1016/j.envres.2017.03.010

Kidd PS, Domínguez-Rodríguez MJ, Díez J, Monterroso C (2007) Bioavailability and plant accumulation of heavy metals and phosphorus in agricultural soils amended by long-term application of sewage sludge. Chemosphere 66:1458–1467. https://doi.org/10.1016/j.chemosphere.2006.09.007

Kong LJ, Han MN, Shih K, Su MH, Diao ZH, Long JY, Chen DY, Hou LA, Peng Y (2018) Nano-rod Ca-decorated sludge derived carbon for removal of phosphorus. Environ Pollut 233:698–705. https://doi.org/10.1016/j.envpol.2017.10.099

Li RD, Zhao WW, Li YL, Wang WY, Zhu X (2015) Heavy metal removal and speciation transformation through the calcination treatment of phosphorus-enriched sewage sludge ash. J Hazard Mater 283:423–431. https://doi.org/10.1016/j.jhazmat.2014.09.052

Lia JP, Gan JH, Hu YJ (2016) Characteristics of heavy metal species transformation of Pb, Cu, Zn from Municipal sewage sludge by Thermal Drying. Procedia Environ Sci 31:961–969. https://doi.org/10.1016/j.proenv.2016.03.001

Pardo P, López-Sánchez JF, Rauret G (2003) Relationships between phosphorus fractionation and major components in sediments using the SMT harmonised extraction procedure. Anal Bioanal Chem 376:248–254. https://doi.org/10.1007/s00216-003-1897-y

Qian TT, Jiang H (2014) Migration of phosphorus in sewage sludge during different thermal treatment processes. ACS Sustain Chem Eng 2:1411–1419. https://doi.org/10.1021/sc400476j

Schwitalla D, Reinmöller M, Forman C, Wolfersdorf C, Gootz M, Bai J, Guhl S, Neuroth M, Meyer B (2018) Ash and slag properties for co-gasification of sewage sludge and coal: an experimentally validated modeling approach. Fuel Process Technol 175:1–9. https://doi.org/10.1016/j.fuproc.2018.02.026

Shi WS, Liu CG, Ding DH, Lei ZF, Yang YN, Feng CP, Zhang ZY (2013) Immobilization of heavy metals in sewage sludge by using subcritical water technology. Bioresour Technol 137:18–24. https://doi.org/10.1016/j.biortech.2013.03.106

Siebielska I (2014) Comparison of changes in selected polycyclic aromatic hydrocarbons concentrations during the composting and anaerobic digestion processes of municipal waste and sewage sludge mixtures. Water Sci Technol 70:1617–1624. https://doi.org/10.2166/wst.2014.417

Stefaniuk M, Oleszczuk P (2016) Addition of biochar to sewage sludge decreases freely dissolved PAHs content and toxicity of sewage sludge amended soil. Environ Pollut 218:242–251. https://doi.org/10.1016/j.envpol.2016.06.063

Walter I, Martínez F, Cala V (2006) Heavy metal speciation and phytotoxic effects of three representative sewage sludges for agricultural. Environ Pollut 139:507–514. https://doi.org/10.1016/j.envpol.2005.05.020

Wang L, Wang C, Ning P, Jiang M, Qin Y (2013) Phosphorus-fixation by hydrated lime in fluidized bed combustion of yellow phosphorus tail gas. J Cent South Univ (Sci and Technol) 44:835–842 (In Chinese)

Wang C, Geng YM, Cheng L, Mao YX (2018) Speciation, mass loading, and fate of phosphorus in the sewage sludge of China. Environ Sci Pollut Res 175:97–103. https://doi.org/10.1007/s11356-018-3520-y

Xu HH, He P, Gu WW, Wang GZ, Shao LM (2012) Recovery of phosphorus as struvite from sewage sludge ash. J Environ Sci-China 24:1533–1538. https://doi.org/10.5004/dwt.2018.22764

Xu GR, Liu MW, Li GB (2013) Stabilization of heavy metals in lightweight aggregate made from sewage sludge and rivers sediment. J Hazard Mater 260:74–81. https://doi.org/10.1016/j.jhazmat.2013.04.006

Zhang J, Yu T, Zhang J (2017) Release of phosphorus from sewage sludge during ozonation and removal by magnesium ammonium phosphate. Environ Sci Pollut Res 24:23794–23802. https://doi.org/10.1007/s11356-017-0037-8